

# Electron and proton heating by solar wind turbulence

B. Breech,<sup>1</sup> W.H. Matthaeus,<sup>2</sup> S.R. Cranmer,<sup>3</sup> J.C. Kasper,<sup>3</sup> and S. Oughton<sup>4</sup>

**Abstract.** Previous formulations of heating and transport associated with strong magnetohydrodynamic (MHD) turbulence are generalized to incorporate separate internal energy equations for electrons and protons. Electron heat conduction is included. Energy is supplied by turbulent heating that affects both electrons and protons, and is exchanged between them via collisions. Comparison to available Ulysses data shows that a reasonable accounting for the data is provided when (i) the energy exchange timescale is very long and (ii) the deposition of heat due to turbulence is divided, with 60% going to proton heating and 40% into electron heating. Heat conduction, determined here by an empirical fit, plays a major role in describing the electron data.

## 1. Introduction

The solar wind displays a highly non-adiabatic temperature profile, requiring some process(es) to provide additional heat sources. One possible, and successful, source of heating comes from magnetohydrodynamic (MHD) turbulence present in the solar wind [Coleman, 1968]. An active MHD turbulent cascade [MacBride et al., 2008; Marino et al., 2008] transfers energy from the large-scale fluctuations down to small scales where kinetic processes dissipate the energy as heat. Previous theories [Zhou and Matthaeus, 1990; Marsch and Tu, 1993; Oughton and Matthaeus, 1995; Zank et al., 1996; Matthaeus et al., 1999; Smith et al., 2001, 2006; Matthaeus et al., 2004; Breech et al., 2005; Isenberg et al., 2003; Breech et al., 2008], have been able to account for radial evolution of fluctuation level, correlation scale, cross helicity and temperature in a specified background solar wind flow. These theories (with some exceptions [e.g., Cranmer et al., 2007]) have focused only on proton temperature, ignoring heat conduction and, in effect, assuming that dissipation of turbulence occurs only through proton kinetic channels. While neglect of proton heat conduction is justified, it is not obvious why all turbulent heating should impact protons alone, nor is it clear why, or whether, proton-electron energy exchange can be neglected.

Electrons provide additional heating by carrying the bulk of the solar wind heat flux and through collisions with the protons. Turbulence models often neglect electrons in favor of the protons as the protons help set the scales of interest. This is particularly clear in the case of the momentum content and the mass density of the solar wind plasma. However the internal energy content of the electrons is not negligible compared to that of the protons.

For this work, we seek to understand how electrons and protons conspire to heat the solar wind. Two possible avenues immediately open up to explore these issues: 1) an empirically based approach to compute the heating rates and 2) a modelling approach based on turbulence theory. A companion paper [Cranmer et al., 2009] follows the first avenue, e.g., examines effects of electrons through a more

empirically based approach. Here we focus on modelling the heating of the solar wind through MHD turbulence theory. For the first time, effects of electron heat conduction are included in a turbulence transport model that extends beyond the inner heliosphere. This provides an important step toward realism and completeness in the turbulent heating models, and enables the use of additional observational constraints.

Under the assumptions of a spherically expanding, radially constant solar wind, the equations for the steady-state temperatures of electrons,  $T_e$ , and protons,  $T_p$ , may be written as

$$\frac{dT_e}{dr} = -\frac{4}{3} \frac{T_e}{r} + \frac{2}{3} \frac{1}{k_B n_e U} Q_e - \frac{T_e - T_p}{U\tau} - \frac{2}{3} \frac{1}{k_B n_e U} \nabla \cdot \mathbf{q}_e, \quad (1)$$

$$\frac{dT_p}{dr} = -\frac{4}{3} \frac{T_p}{r} + \frac{2}{3} \frac{1}{k_B n_p U} Q_p + \frac{T_e - T_p}{U\tau}, \quad (2)$$

where  $r$  is heliocentric distance,  $U$  is the bulk solar wind speed,  $n_{\{e,p\}}$  is the electron (proton) number density,  $Q_{\{e,p\}}$  represents turbulent heating per unit mass,  $\mathbf{q}_e$  is the electron heat flux vector (proton heat flux vector has been neglected), and  $k_B$  is Boltzmann's constant. The  $T_e - T_p$  terms in Eqs. (1)–(2) model Coulomb collisions taking place over a timescale  $\tau$  [e.g., Priest, 1982].

In previous models [Zank et al., 1996; Matthaeus et al., 1999; Smith et al., 2001; Breech et al., 2008] the equation for evolution of the temperature has been supplemented by an equation for the turbulence energy, an equation for the correlation or energy-containing scale and an equation for the cross helicity. These will be revisited further below. Here we will focus on issues surrounding the inclusion of the separate temperature equations for protons and electrons. In particular, three questions arise by writing down these equations: (1) How does the electron heat flux vary with distance? (2) How much turbulent dissipation goes into heating the electrons versus the protons? and (3) Over what timescale do the electrons and protons experience energy exchange couplings, such as Coulomb collisions, that tend to equilibrate their temperatures?

In this paper, we explore the physical issues surrounding these questions within the context of a turbulence transport model for the solar wind. The physical issues may be further complicated by the effects of pickup protons and latitudinal variations present in the solar wind. As a result, we limit ourselves to the high latitude fast wind, which displays less dependence on latitude, at least above 35 degrees or so [McComas et al., 2000]. We also limit ourselves to examining these issues primarily in the inner parts of the heliosphere ( $r < 10$  AU), which avoids complications due to pickup protons. In future work, we will examine how pickup protons and latitudinal variations affect the key issues listed above.

<sup>1</sup>NASA Goddard Space Flight Center

<sup>2</sup>Department of Physics and Astronomy and Bartol Research Institute, University of Delaware

<sup>3</sup>Harvard-Smithsonian Center for Astrophysics

<sup>4</sup>Department of Mathematics, University of Waikato, Hamilton, New Zealand

## 2. Electron Effects

### 2.1. Electron Heat Flux

One of the new effects we include is the electron heat flux. Generally speaking the heat flux associated with the proton distribution is regarded as unimportant [Braginskii, 1965]. For the case of the solar wind, a simple way to see this is to assume that the proton heat flux is due to a beam with fractional number density,  $f_{\text{beam}}$ , moving at the Alfvén speed,  $V_A$ , relative to the bulk proton population. This leads to a heat flux on the order of  $f_{\text{beam}} V_A^3$ . If we take the scale of its divergence to be  $R$ , the heliocentric distance, then the relative contribution of the divergence of the proton heat flux to the proton temperature given in Eq. (2) is of the order  $f_{\text{beam}} V_A^3 / R$ . We compare this result to the heating term (see §2.3 below), which is of order  $Z^3 / \lambda$ , where  $Z$  is the fluctuation amplitude and  $\lambda$  the correlation scale. Since  $Z \sim V_A / 2$  and  $\lambda \sim R / 100$ , while  $f_{\text{beam}}$  cannot be greater than unity and is probably  $< 1/10$ , it is clear that for protons the heat flux is much less important than the heating. Electrons, on the other hand, with their high thermal speed and anisotropic distribution functions, are affected greatly by heat flux. Within the solar wind, the electron heat flux is primarily along the magnetic field. Heat flux transverse to the magnetic field is severely reduced as the magnetic field effectively acts as an insulating blanket.

Modeling  $q_{\parallel}$ —the electron heat flux along the magnetic field—requires approximating the solar wind as either collision dominated or collisionless. A collision dominated model,  $q_{\parallel} = -\kappa_{\parallel} \nabla_{\parallel} T_e(r)$  [Spitzer and Härm, 1953] produces temperatures that are too large at 1 AU compared to observations [Hollweg, 1976]. Collisionless models [Hollweg, 1976] fare much better and may be adequate for most purposes. Nonetheless, the collisionless models can still suffer from missing non-local effects [Canullo et al., 1996; Scudder and Olbert, 1979].

Rather than employing a theoretically based model, here we adopt a more empirical approach in order to handle these difficulties in specifying  $q_{\parallel}$ . We derive  $q_{\parallel}$  from observational data by applying a best fit procedure to the electron heat fluxes given by Pilipp et al. [1990] for 0.3 AU to 1 AU and Scime et al. [1994] for 1 AU to 5.4 AU. Figure 1 shows the observations and the fitted curve. Introducing  $x \equiv \log_{10}(r/R_{1\text{AU}})$ , the final fit is given by

$$\log_{10} q_{\parallel}(r) = -2.3054 - 2.115x - 0.58604x^2, \quad (3)$$

and is assumed to be a reasonable approximation out to  $r \sim 100$  AU. Note that past 10 AU, pickup proton effects may invalidate this assumption.

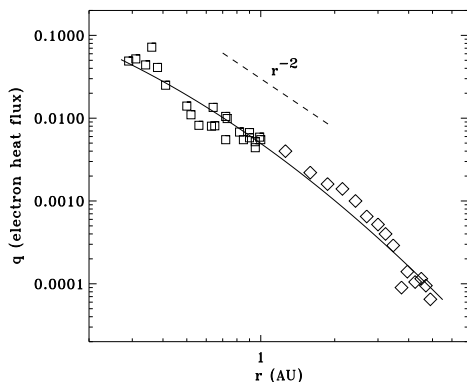


**Figure 1.** Observed electron heat flux (cgs units) [Pilipp et al., 1990; Scime et al., 1994] and fits to the data.

We remark that the use of this electron heat conduction data may introduce some uncertainty into our results. In particular, the measurements shown in Figure 1 were adopted from Scime et al. [1994]. The observations come from the initial Ulysses cruise phase from 1 to 5 AU, while Ulysses was in the ecliptic plane. To our knowledge, no velocity selection was performed on the observations. We therefore assume the measurements apply to all wind speed intervals and latitudes. Note that in some later observations, Scime et al. [1999] found no significant variation in  $q_{\parallel}$  at higher latitudes, which are dominated by the fast wind. We will return to this point later when discussing our results.

### 2.2. Collision Effects

Protons and electrons can exchange heat through Coulomb collisions, though they may do so over extremely long timescales. They each can also exchange energy with the electromagnetic field, and therefore indirectly with each other, through wave-particle interactions. These kinetic effects may be thought of as producing effective collisions. The observational fact that protons and electrons frequently maintain different temperatures in the solar wind [Hundhausen, 1972] provides clear evidence that this coupling is not very strong. Generally, the scales for observing collisional effects correspond to several AU, as has been found recently [Kasper et al., 2008] in a comparison of fast and slow wind characteristics where proton-ion collisions are the central consideration.

Taking into account this background, we adopt a (somewhat) arbitrary approach for setting the collision timescale,  $\tau$ . For this work, we set  $\tau$  as a constant equal to the plasma transit time to some distance (e.g., 10 AU). This choice produces only a weak interaction between protons and electrons, but does allow for collisional energy exchange effects to be seen in the model results.

### 2.3. Partitioning Turbulent Heating

As the solar wind plasma evolves, MHD turbulence transfers energy from low wavenumbers to high wavenumbers, where the energy is dissipated. The dissipated energy heats both the protons and electrons. Since we are modeling the supply of energy from large scales to small scales, a process believed to be controlled mainly by large-scale MHD processes, we cannot, on the basis of this analysis, distinguish the channel or sequence of kinetic processes that absorbs the energy. Possibilities are kinetic Alfvén waves [Leamon et al., 1998; Cranmer and van Ballegoijen, 2003; Bale et al., 2005; Gary and Borovsky, 2008], whistlers [Gary et al., 2008], and nonlinear dissipation in current sheets [Sundkvist et al., 2007], to name a few. To account for the data, however, we will have to employ a reasonably correct partitioning of the cascaded energy into the heat functions  $Q_p$  and  $Q_e$  that appear in the temperature equations (1) and (2).

Specifically, let  $Q$  be the total energy dissipated by the turbulence. We then define

$$Q_p \equiv f_p Q, \quad Q_e \equiv (1 - f_p) Q, \quad (4)$$

where  $f_p$  is the fraction that determines the amount of turbulent heating that goes into the protons ( $Q_p$ ). The rest of the heat is given to the electrons ( $Q_e$ ). We make no distinction here between the core, halo, and strahl populations of the electrons as the turbulence heats all electrons.

In principle,  $f_p$  can be determined by the underlying kinetic physics [Gary and Borovsky, 2004], which operates at scales far smaller than the energy-containing scale described by the turbulence model.  $f_p$  may also change with increasing distance [see the companion paper Cranmer et al., 2009, for

more details on how  $f_p$  may change]. We neglect these features of the problem for now and simply adopt  $f_p = \text{const}$ .

Some evidence suggests [Leamon *et al.*, 1998, 1999] that  $f_p \approx 0.60$  at 1 AU, if one associates helicity-sensitive processes with proton cyclotron absorption, and the remaining heating as due to a process like Landau damping, which can affect both protons and electrons. There has also been the suggestion [Matthaeus *et al.*, 2008] that a stronger cascade drives proton instabilities more robustly, leading to more absorption near proton cyclotron scales. However, lacking a firm quantitative theoretical basis, such empirically based arguments must be regarded with caution at present. Therefore we revert to a purely empirical choice of  $f_p$ , to be supported or contraindicated by the results of the model, shown below.

For the total heating rate due to the cascade,  $Q$ , we employ a *von Kármán and Howarth* [1938] style phenomenology giving

$$Q \sim \frac{Z^3}{\lambda} \quad (5)$$

with  $Z^2$  being (twice) the total energy available to the turbulence and  $\lambda$  being the length scale of the largest turbulent structures. Both of these quantities must be extracted from the turbulence model. Note that this dissipation model is rather robust and has been successfully applied to very different regimes, such as the super Alfvénic solar wind [e.g., Breech *et al.*, 2008] and the corona [e.g., Dmitruk *et al.*, 2001; Verdini and Velli, 2007].

### 3. Turbulence Model

We adopt the following turbulence model [Zank *et al.*, 1996; Matthaeus *et al.*, 1999, 2004; Smith *et al.*, 2001, 2006; Isenberg *et al.*, 2003; Breech *et al.*, 2005, 2008] which comprises three equations describing the transport of turbulence quantities; one equation for (twice) the total turbulent energy,  $Z^2$ ,

$$\frac{dZ^2}{dr} = -\frac{Z^2}{r} + \frac{C_{\text{sh}} - M\sigma_D}{r} Z^2 + \frac{\dot{E}_{PI}}{U} - \alpha f^+ \frac{Z^3}{\lambda U}, \quad (6)$$

correlation (similarity) scale,  $\lambda$ ,

$$\frac{d\lambda}{dr} = \beta f^+ \frac{Z}{U} - \frac{\beta}{\alpha} \frac{\dot{E}_{PI}}{U Z^2} \lambda, \quad (7)$$

and the normalized cross helicity,  $\sigma_c$ ,

$$\frac{d\sigma_c}{dr} = \alpha f' \frac{Z}{U \lambda} - \left[ \frac{C_{\text{sh}} - M\sigma_D}{r} + \frac{\dot{E}_{PI}}{U Z^2} \right] \sigma_c, \quad (8)$$

where

$$f^\pm(\sigma_c) = \frac{(1 - \sigma_c^2)^{1/2}}{2} \left[ (1 + \sigma_c)^{1/2} \pm (1 - \sigma_c)^{1/2} \right], \quad (9)$$

and  $f'(\sigma_c) = \sigma_c f^+ - f^-$ . Driving of the turbulence comes from shear, modeled through  $C_{\text{sh}}$ , and pickup protons,  $\dot{E}_{PI}$ , with shear being more dominant in the inner heliosphere (say,  $r < 10$  AU) and pickup protons more dominant in the outer heliosphere.  $M = 1/2$  relates to the underlying turbulence geometries and  $\sigma_D = -1/3$  approximates the normalized energy difference (kinetic minus magnetic) of the fluctuations. More details on the model itself, and its parameters, can be found in Breech *et al.* [2008].

The rightmost term of Eq. (1),  $\alpha f^+ Z^3 / \lambda U$ , controls the turbulent dissipation. The constant  $\alpha$  (taken =  $2\beta$  herein) modulates the efficiency of the dissipation, with higher values resulting in a more efficient dissipation (e.g., more active turbulent cascade). Previous use of the turbulent model [such as Breech *et al.*, 2008; Smith *et al.*, 2006] used values

of  $\alpha = 0.8$ . For this work, we adopt lower values of  $\alpha = 0.5$  based on the results of hydrodynamical simulations [Pearson *et al.*, 2004]. Even lower values, down to  $\alpha = 1/8$ , may also be consistent with those simulations.

The turbulence dissipates energy, which then goes into heating of the solar wind and manifests as elevated electron and proton temperatures. The total turbulence heating rate is given as

$$Q = \frac{1}{2} \alpha \rho f^+(\sigma_c) \frac{Z^3}{\lambda} \quad (10)$$

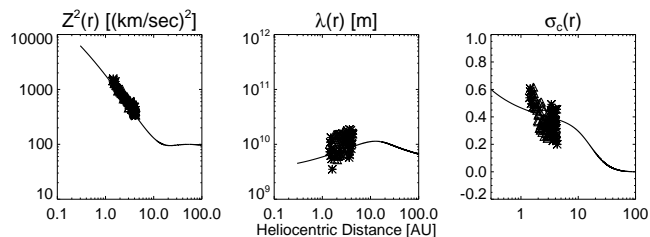


**Figure 2.** Solution of the turbulence model used in this paper. The boundary values are specified at 0.3 AU as  $Z^2 = 5000 \text{ (km/s)}^2$ ,  $\lambda = 0.03 \text{ AU}$ , and  $\sigma_c = 0.6$ . Other parameters are set as  $U = 774 \text{ km/s}$ ,  $C_{\text{sh}} = 0.25$ ,  $\alpha = 2\beta = 0.5$ , and  $M\sigma_D = -1/6$ . Pickup protons effectively turn on near 10 AU. The solutions (solid lines) compare reasonably well to the observed Ulysses values from near solar minimum [Bavassano *et al.*, 2000a, b].

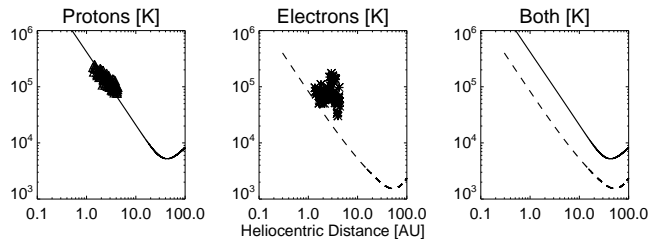


**Figure 3.** Model solutions for the proton and electron temperatures computed without collisions and without electron heat conduction. The proton solution matches the observations well, but the electron solution misses almost all of the observed data.

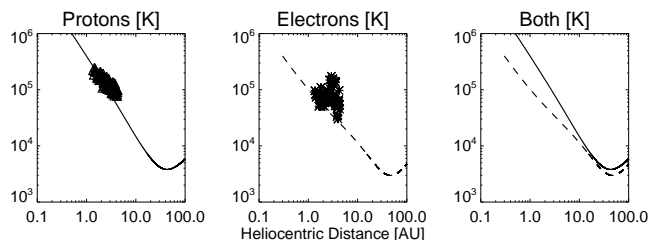


**Figure 4.** Model solutions for the proton and electron temperatures computed with collisions but without electron heat conduction. The proton solution is reasonable, but the electron solution falls below most of the observed data. Collisional effects are also apparent, with the two temperatures beginning to equalize in the outer heliosphere, although the protons stay warmer.

which is partitioned between the electrons and protons according to Eq. (4). The factor of  $1/2$  appears because  $Z^2$  is twice the energy density of the fluctuations.

#### 4. Model Results

We can numerically solve the transport model, Eqs. (1)–(8), and use the results to compute the temperature values. Figure 2 shows the solutions of the turbulence model. The computed solutions compare well against Ulysses observations of 1 hour cadence from solar minimum [Bavassano *et al.*, 2000a, b]. The model can also produce other solutions, which bracket the observed values [see Breech *et al.*, 2008].

The transport solutions can then be used to compute the proton and electron temperatures using Eqs. (1) and (2) and taking  $f_p$  as a constant 0.6. The temperature solutions given below use observations from the SWOOPS [Bame *et al.*, 1992] experiment on Ulysses corresponding to the same time as the observations shown in Fig. 2. The temperature observations were made in the high latitude, fast wind during solar minimum conditions. For the proton temperatures, we have used the geometric mean of the two temperature values given in the data archives [see Cranmer *et al.*, 2009, for more information]. For the electron temperatures, SWOOPS provides temperature data for the core, halo, and total electron populations. We compare our results against the total electron temperature as the turbulence heating should affect all

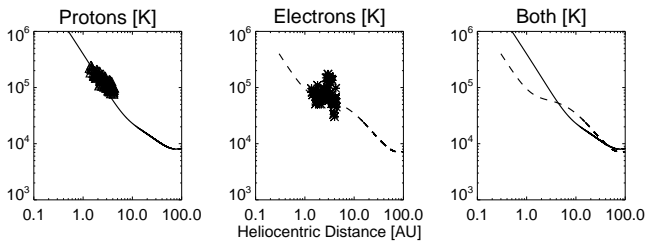


**Figure 5.** Model solutions for the proton and electron temperatures computed with both collisions and electron heat conduction turned on. The proton solution remains reasonable. The electron solution displays a “shelf-like” region between 1 and 10 AU. The solution matches the observations better than not including the heat conduction (cf. Fig. 4).

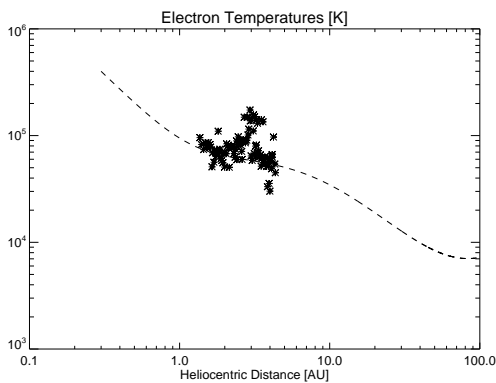


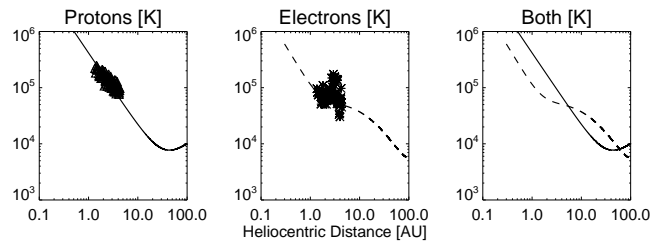
**Figure 6.** The electron temperature solution from Figure 5 showing the “shelf” region more clearly. The solution fits most of the data, although there are outliers, particularly around 3 AU. The “shelf” region is due to heat conduction (see text).

electrons. For the model solutions, we take the initial values of  $T_p = 2.0 \times 10^6$  K and  $T_e = 4.0 \times 10^5$  K at 0.3 AU.

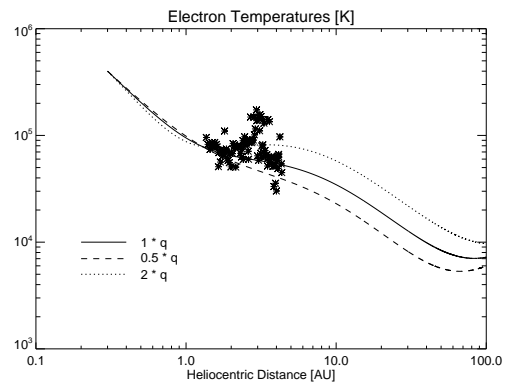
Figure 3 displays the temperature solutions without heat conduction and almost without collisions. The collision timescale  $\tau$  was set equal to the time for plasma to transit to 100 AU, which effectively removes collision effects from the results. The proton solution agrees very well with the observed data, but the electron solution misses almost all the data.

Figure 4 shows the temperature solutions without the electron heat conduction, but with collisions turning on at 10 AU (i.e.,  $\tau$  was set to the transit time to 10 AU). The proton solution mostly agrees with the observations, but does show some disagreement near 5 AU where the proton temperature solution is slightly cooler than the observations indicate. Collisions evidently cause the slight disagreement as this disagreement is not present in Fig. 3. This may provide evidence that setting the collision time to be the transit time to 10 AU is too low a value.

In contrast to the proton temperature solution, the electron solution becomes slightly better when collisions are included. The energy lost from the protons profits the electrons. Nonetheless, the electron solution still misses most of the observed data.



**Figure 7.** Model solutions for the proton and electron temperatures computed with electron heat conduction turned on, but without collisions. The shelf in the electron temperature solution is still present, as is the crossover of the electron and proton solutions. The initial value of the electron temperature was raised to  $6.0 \times 10^5$  K to maintain the good agreement with observations.



**Figure 8.** Solutions for the electron temperature using different profiles of the heat flux vector,  $q_{\parallel}$ . The baseline solution uses the heat flux vector given in Eq. (3). The other two solutions use baseline heat flux multiplied by 2 and divided by 2. Possible variations in the heat flux should be encompassed by those two extremes. The figure demonstrates that a higher heat flux will make the shelf region more pronounced, while a lower heat flux lessens the shelf.

Including both electron heat conduction, as determined from equation (3), and collisions produces interesting results (Fig. 5). The electron temperature now features a “shelf” region between 1 and 10 AU where  $T_e(r)$  does not decrease as rapidly as it does outside that region. Interestingly, the electron temperature solution crosses the proton temperature solution near 5 AU, after which the electrons are actually warmer than the protons. Collisions then begin to take hold, resulting in higher proton temperatures and lower electron temperatures.

Figure 6 shows only the electron solution from Figure 5. The shelf region matches the observed electron temperatures better than the solutions obtained when heat conduction is neglected. While there is some variability in the observations, the solution goes through most of the available data. Within this region, the heat conduction evidently allows some heat to “pile up” to allow the electrons to stay warmer than they may otherwise be. The shelf arises from the electron heat flux shifting from a form close to  $r^{-2}$  to a steeper form in the outer heliosphere.

We note that the existence of the shelf region must be handled carefully. The shelf originates from the model solutions and compares favorably with the data we have. However, no high latitude data is available beyond about 5 AU. Further data would be required to confirm the existence of shelf. Additionally, while we chose the electron temperature data to match published data sets [Bavassano et al., 2000a, b], it may be possible that there are data selection effects that lead to the appearance of the shelf. The temperature data itself was taken solar minimum conditions and has a cadence of 1 hour. Selecting data with other cadences or different solar cycle conditions could easily obscure the shelf [see, for instance, Phillips et al., 1995].

The shelf is due solely to electron heat conduction, as Fig. 7 reveals. For the solutions shown there, collisions were turned off (i.e.,  $\tau$  is set to the transit time to 100 AU). The shelf is still present, although the initial value of the electron temperature had to be increased from  $4.0 \times 10^5$  K (as in the other solutions) to  $6.0 \times 10^5$  K to maintain similar agreement with the observations. Note that the proton solution displays better agreement with the observations due to the lack of collisions.

The shelf is somewhat sensitive to the underlying electron heat flux vector,  $q_{\parallel}$ , used to compute the solutions. Figure 8 shows the electron temperature solutions computed using three different profiles for  $q_{\parallel}$ . Equation (3) provides the baseline profile, which yields the electron temperature solution shown in Figure 6). The other two solutions use a heat flux vector where the baseline  $q_{\parallel}$  was multiplied by 2 and divided by 2. Since Scime et al. [1999] found small variations in the heat flux with latitude, any variation in the heat flux measurements should lie between these two extremes. The electron temperature solutions show that increasing the heat flux makes the shelf more pronounced. Lowering the heat flux lessens the shelf.

## 5. Conclusions

For this work, we have added the effects of electrons to a turbulence transport model for the solar wind. Electron effects manifest in the division of turbulent heating between protons and electrons, collisions between protons and electrons, and heat conduction of the electrons. We find that adding an empirical model for electron heat conduction makes a dramatic difference in the solutions. A “shelf-like” region appears between 1 and 10 AU where the electron temperatures do not decrease as rapidly as they do outside that region. The electrons stay warm enough to actually become warmer than the protons. Observations of the electron temperatures seem to support the presence of the shelf. We also find that collisions between the protons and electrons may not be important until well past 10 AU. Allowing collisions to take effect closer in appears to cause discrepancies between the model’s proton temperature solution and observed data.

**Acknowledgments.** This research was supported in part by an appointment to the NASA Postdoctoral Program at Goddard Space Flight Center, administered by Oak Ridge Associated Universities through a contract with NASA. SRC’s work was supported by the National Aeronautics and Space Administration (NASA) under grants NNG04GE77G, NNX06AG95G, and NNX09AB27G to the Smithsonian Astrophysical Observatory. WHM’s work was supported by NSF ATM 0752135 (SHINE) and NASA NNX08AI47G (Heliophysics Theory Program). JCK’s work was supported by NASA grant NNX08AW07G.

## References

- Bale, S. D., P. J. Kellogg, F. S. Mozer, T. S. Horbury, and H. Reme, Measurement of the electric fluctuation spectrum of magnetohydrodynamic turbulence, *Phys. Rev. Lett.*, *94*, 215002, doi:10.1103/PhysRevLett.94.215002, 2005.
- Bame, S., D. McComas, B. Barraclough, K. Sofaly, J. Chavez, B. Goldstein, and R. Sakurai, The Ulysses solar wind plasma experiment, *Astron. Astrophys. Supp.*, *92*, 237–265, 1992.
- Bavassano, B., E. Pietropaolo, and R. Bruno, Alfvénic turbulence in the polar wind: A statistical study on cross helicity and residual energy variations, *J. Geophys. Res.*, *105*, 12697–12704, 2000a.
- Bavassano, B., E. Pietropaolo, and R. Bruno, On the evolution of outward and inward Alfvénic fluctuations in the polar wind, *J. Geophys. Res.*, *105*, 15959–15964, 2000b.
- Braginskii, S. I., Transport processes in a plasma, *Rev. Plasma Phys.*, *1*, 205, 1965.
- Breech, B., W. H. Matthaeus, J. Minnie, S. Oughton, S. Parhi, J. W. Bieber, and B. Bavassano, Radial evolution of cross helicity in high-latitude solar wind, *Geophys. Res. Lett.*, *32*, L06103, doi:10.1029/2004GL022321, 2005.
- Breech, B., W. H. Matthaeus, J. Minnie, J. W. Bieber, S. Oughton, C. W. Smith, and P. A. Isenberg, Turbulence transport throughout the heliosphere, *J. Geophys. Res.*, *113*, A08105, doi:10.1029/2007JA012711, 2008.
- Canullo, M. V., A. Costa, and C. Ferro-Fontan, Nonlocal heat transport in the solar wind, *Astrophys. J.*, *462*, 1005–1010, 1996.
- Coleman, P. J., Turbulence, viscosity, and dissipation in the solar wind plasma, *Astrophys. J.*, *153*, 371–388, 1968.
- Cranmer, S., W. Matthaeus, B. Breech, and J. Kasper, Empirical constraints on proton and electron heating in the inner heliosphere, *submitted to ApJ*, 2009.
- Cranmer, S. R., and A. A. van Ballegoijen, Alfvénic turbulence in the extended solar corona: Kinetic effects and proton heating, *Astrophys. J.*, *594*, 573–591, 2003.
- Cranmer, S. R., A. A. van Ballegoijen, and R. Edgar, Self-consistent coronal heating and solar wind acceleration from anisotropic magnetohydrodynamic turbulence, *Astrophys. J. Suppl. Ser.*, *171*, 520–551, doi:10.1086/518001, 2007.
- Dmitruk, P., L. J. Milano, and W. H. Matthaeus, Wave-driven turbulent coronal heating in open field line regions: Nonlinear phenomenological model, *Astrophys. J.*, *548*, 482–491, 2001.
- Gary, S. P., and J. E. Borovsky, Alfvén-cyclotron fluctuations: Linear Vlasov theory, *J. Geophys. Res.*, *109*(A18), 6105, doi:10.1029/2004JA010399, 2004.
- Gary, S. P., and J. E. Borovsky, Damping of long-wavelength kinetic Alfvén fluctuations: Linear theory, *J. Geophys. Res.*, *113*(A12), 12,104, doi:10.1029/2008JA013565, 2008.
- Gary, S. P., S. Saito, and H. Li, Cascade of whistler turbulence: Particle-in-cell simulations, *Geophys. Res. Lett.*, *35*, 2104, doi:10.1029/2007GL032327, 2008.
- Hollweg, J. V., Collisionless electron heat conduction in the solar wind, *J. Geophys. Res.*, *81*, 1649–1658, 1976.
- Hundhausen, A. J., *Coronal Expansion and the Solar Wind*, Springer-Verlag, New York, 1972.
- Isenberg, P. A., C. W. Smith, and W. H. Matthaeus, Turbulent heating of the distant solar wind by interstellar pickup protons, *Astrophys. J.*, *592*, 564–573, 2003.

- Kasper, J. C., A. J. Lazarus, and S. P. Gary, Hot solar-wind Helium: Direct evidence for local heating by Alfvén - Cyclotron dissipation, *Phys. Rev. Lett.*, *101*(26), 261103, doi: 10.1103/PhysRevLett.101.261103, 2008.
- Leamon, R. J., W. H. Matthaeus, C. W. Smith, and H. K. Wong, Contribution of cyclotron-resonant damping to kinetic dissipation of interplanetary turbulence, *Astrophys. J.*, *507*, L181, 1998.
- Leamon, R. J., C. W. Smith, N. F. Ness, and H. K. Wong, Dissipation range dynamics: Kinetic Alfvén waves and the importance of  $\beta_e$ , *J. Geophys. Res.*, *104*, 22331, 1999.
- MacBride, B. T., C. W. Smith, and M. A. Forman, The turbulent cascade at 1 AU: Energy transfer and the third-order scaling for MHD, *Astrophys. J.*, *679*(2), 1644–1660, doi: 10.1086/529575, 2008.
- Marino, R., L. Sorriso-Valvo, V. Carbone, A. Noullez, R. Bruno, and B. Bavassano, Heating the solar wind by a magnetohydrodynamic turbulent energy cascade, *Astrophys. J.*, *677*, L71–L74, doi:10.1086/587957, 2008.
- Marsch, E., and C.-Y. Tu, Modeling results on spatial transport and spectral transfer of solar wind Alfvénic turbulence, *J. Geophys. Res.*, *98*, 21045, 1993.
- Matthaeus, W. H., G. P. Zank, C. W. Smith, and S. Oughton, Turbulence, spatial transport, and heating of the solar wind, *Phys. Rev. Lett.*, *82*, 3444–3447, doi: 10.1103/PhysRevLett.82.3444, 1999.
- Matthaeus, W. H., J. Minnie, B. Breech, S. Parhi, J. W. Bieber, and S. Oughton, Transport of cross helicity and the radial evolution of Alfvénicity in the solar wind, *Geophys. Res. Lett.*, *31*, L12803, doi:10.1029/2004GL019645, 2004.
- Matthaeus, W. H., J. M. Weygand, P. Chuychai, S. Dasso, C. W. Smith, and M. G. Kivelson, Interplanetary magnetic Taylor microscale and implications for plasma dissipation, *Astrophys. J.*, *678*, L141–L144, doi:10.1086/588525, 2008.
- McComas, D. J., et al., Solar wind observations over Ulysses' first full polar orbit, *J. Geophys. Res.*, *105*, 10419–10434, 2000.
- Oughton, S., and W. H. Matthaeus, Linear transport of solar wind fluctuations, *J. Geophys. Res.*, *100*, 14783–14799, 1995.
- Pearson, B. R., T. A. Yousef, N. E. L. Haugen, A. Brandenburg, and P.-A. Krogstad, Delayed correlation between turbulent energy injection and dissipation, *Phys. Rev. E*, *70*, 056301, doi: 10.1103/PhysRevE.70.056301, 2004.
- Phillips, J. L., S. J. Bame, S. P. Gary, T. Gosling, E. E. Scime, and R. J. Forsyth, Radial and meridional trends in solar wind thermal electron temperature and anisotropy: Ulysses, *Space Sci. Rev.*, *72*, 109, 1995.
- Pilipp, W., H. Miggenrieder, K. Mühlhäuser, H. Rosenbauer, and R. Schwenn, Large-scale variations of thermal electron parameters in the solar wind between 0.3 and 1 AU, *J. Geophys. Res.*, *95*, 6305–6329, 1990.
- Priest, E. R., *Solar Magnetohydrodynamics*, Reidel, Dordrecht, Holland, 1982.
- Scime, E. E., S. J. Bame, W. C. Feldman, S. P. Gary, J. L. Phillips, and A. Balogh, Regulation of the solar wind electron heat flux from 1 to 5 AU: Ulysses observations, *J. Geophys. Res.*, *99*, 23401–23410, 1994.
- Scime, E. E., A. E. B. Jr, and J. Littleton, The electron heat flux in the polar solar wind: Ulysses observations, *Geophys. Res. Lett.*, *26*(14), 2129–2132, 1999.
- Scudder, J. D., and S. Olbert, A Theory of Local and Global Processes which affect Solar Wind Electrons 1. The Origin of Typical 1 AU Velocity Distribution Functions—Steady State Theory, *J. Geophys. Res.*, *84*, 2755–2772, 1979.
- Smith, C. W., W. H. Matthaeus, G. P. Zank, N. F. Ness, S. Oughton, and J. D. Richardson, Heating of the low-latitude solar wind by dissipation of turbulent magnetic fluctuations, *J. Geophys. Res.*, *106*, 8253–8272, 2001.
- Smith, C. W., P. A. Isenberg, W. H. Matthaeus, and J. D. Richardson, Turbulent heating of the solar wind by newborn interstellar pickup protons, *Astrophys. J.*, *638*, 508–517, 2006.
- Spitzer, L., and R. Härm, Transport phenomena in a completely ionized gas, *Phys. Rev.*, *89*(5), 977–981, 1953.
- Sundkvist, D., A. Retino, A. Vaivads, and S. D. Bale, Dissipation in turbulent plasma due to reconnection in thin current sheets, *Phys. Rev. Lett.*, *99*, 025004, doi: 10.1103/PhysRevLett.99.025004, 2007.
- Verdini, A., and M. Velli, Alfvén waves and turbulence in the solar atmosphere and solar wind, *Astrophys. J.*, *662*, 669–676, 2007.
- von Kármán, T., and L. Howarth, On the statistical theory of isotropic turbulence, *Proc. Roy. Soc. London Ser. A*, *164*, 192–215, 1938.
- Zank, G. P., W. H. Matthaeus, and C. W. Smith, Evolution of turbulent magnetic fluctuation power with heliocentric distance, *J. Geophys. Res.*, *101*, 17093, 1996.
- Zhou, Y., and W. H. Matthaeus, Transport and turbulence modeling of solar wind fluctuations, *J. Geophys. Res.*, *95*, 10291, 1990.